Periodica Polytechnica
Civil Engineering

61(2), pp. 232–243, 2017
https://doi.org/10.3311/PPci.9153

RESEARCH ARTICLE

An Improved Ant Colony Algorithm for the Optimization of Skeletal Structures by the Proposed Sampling Search Space Method

Vahid Reza Kalatjari[1], Mohammad Hosein Talebpour[1,2*]

Received 08 March 2016; Revised 22 July 2016; Accepted 04 August 2016

Abstract

Designing space is dramatically enlarged with optimization of structures based on ACO, regard to increasing section's list. This problem decreases the speed of optimization in order to reach to optimum point and also increases local optimum probability, because determining suitable cross section process for each design variable in ACO depends on number of members in the list of section. Therefore, this paper by using partitioning the design space tries to decrease the probability of achieving local optimum during the process of structures optimum design by ACO and to increase the speed of convergence. In this regard, the list of section is divided to specific number of subsets inspired by meshing process in finite element. Then a member of each subset (in three case, maximum, middle and minimum of cross section) is defined as a representative of subset in a new list. Optimization process starts based on the new lit of section (global search). After specific number of repetitions, optimum design range for each variable will be determined. Afterward, variable section list is defined for each design variable related to result of previous step of process and based on subset of related variable. Finally, optimization process is continued based on the new list of section for each design variable to the end of process (local search). Proposal is studied in three cases and compared with common method in ACO and standard optimization examples in skeletal structures are used. Results show an increase in accuracy and speed of optimization according to cross section middle method (Case 2).

Keywords

Structural Optimization, Ant Colony Algorithm, Sampling Design Space

[1] Department of Civil Engineering, Shahrood University of Technology, Shahrood, Iran

[2] School of Engineering, Damghan University, Damghan, Iran

[*] Corresponding author email: m.h.talebpour@du.ac.ir

1 Introduction

One of the important problems in the design of skeletal structures is finding the smallest value of cross sections for each member of structure based on the problem constraints. To this end, various methods have been proposed for optimization of structures. An important category of such methods includes methods known as the meta-heuristic algorithms, which are intelligent random search procedures for searching the design space using different points (i.e. various designs). The logic of these algorithms is such that they require generation of several improved designs during the optimization process.

Ant colony algorithm is known as an efficient meta-heuristic method with good performance [1, 2]. This method was first introduced by Colorni et al. [3, 4] as Ant System (AS) to solve the travelling salesman problem. The main logic of the method was based on the inspiration of ants' behaviour searching for food. Ants as social blind insects live in a society with mutual cooperation and use a chemical substance called pheromone to discover the shortest route towards the food source. Each insect leaves a small amount of pheromone from place to place to identify the way back and also facilitate the route determination for the other ants and return to formicary from the previous route. The more the pheromone of a route, the greater chance for other ants to choose the same route. Consequently, the path to reach the food source may have a greater chance to reinvest the pheromone and also be chosen by other ants. Pheromone rate of each path constantly changes proportional to the passing rate of the other ants and also by the magnitude of the evaporation. Evaporation process results in eliminating the long and unsuccessful routes during ants search action so that the shortest path to the food source will be detected by ants. Inspired by this fact, structural optimization problem was investigated by several research and in some cases the standard algorithm is improved through some enhancements [5–11]. In this relation, different approaches based on Ant Colony algorithm principles namely, Ant Colony System (ACS), Max-Min Ant System (MMAS), Rank-Based Ant System (RBAS), Best and Worst Ant System (BWAS) were proposed by different researchers [13–16].

Examination of the method proposed by researchers for selecting the cross sections for each design variable in different ant colony optimization (ACO) algorithms showed that increases the number of sections leads to a decrease in the convergence speed of the ant colony algorithm and increases the probability of getting trapped in local optimum. In other words, with increases the number of sections, the number of options for each design variable grows. On the other hand, as a result of the increase in the number of sections, the best state for each design variable has a very low probability of selection as compared to other states. Hence, plenty of iterations are required to increase the probability of selection of the best state in relation to the pheromone, and to make a distinction between this state and other possible states for each design variable. Therefore, increases the number of sections plays a significant role in the convergence speed and precision of optimal solution in the ant colony algorithm.

In this paper, first the method for optimizing structures based on the ant colony algorithm was discussed. Afterwards, inspired by the finite elements method, an idea was proposed for meshing the design space to increase convergence speed and precision of the optimal solution in optimization problems. According to this idea, the design space, which is defined in accordance with the list of sections, is divided into smaller parts (i.e. meshing), and the optimization process is run in the first phase based on the selected parts representative. In the literature of the proposed idea, this phase is defined as the global search phase. Afterwards, in the second phase, the search space for each design variable is defined in accordance with results of phase one and the optimization process continue to run. It is worth mentioning that in the global search phase, the methods for dividing and selecting a representative for each part are different, but in this paper three possible cases were introduced and discussed. Finally, examples of skeletal structures were used to compare the performance and potential of the proposed idea with the simple ant colony optimization algorithm. For each case of the proposed idea and the simple colony algorithm, 40 independent and consecutive runs were used. In the end, the average of 40 runs for each case is shown as the graph of the convergence trend for the concerning case. Results show increases the convergence speed due to the cases of the proposed idea.

2 Structural Optimization based on ACO

As mentioned, various methods have been proposed by researchers based on the ant colony algorithm. All of these methods have the same basis and only differ in the suggestions they provide for increasing ACO efficiency. In this paper, the ant colony algorithm used in [1], [7] was employed. This algorithm provides an efficient and improved ACO procedure. Based on [7], during the optimization process, the local search procedure is run by making changes to the pheromone of some members in the list of section. Fig. 1 illustrates the flowchart of the ACO algorithm used in this research.

2.1 Formulation of optimization problem

Formulation of optimization problem of skeletal structures is defined as following:

Find the least value of the weight objective function under the constraints C1 and C2:

$$W(A) = \sum_{i=1}^{Ne} (\rho_i \ell_i a_i) \tag{1}$$

$$C1 : \sigma_j \le \sigma_{all(Ten)} \ , \ |\sigma_j| \le |\sigma_{all(Com)}| \quad j = 1,2,\ldots,Ne \tag{2}$$

$$C2 : |\Delta_k| \le |\Delta_k^{max}| \quad k = 1,2,\ldots,Ndof \tag{3}$$

In Eq. (1), a vector of cross section variables, the matrix [A], is defined as:

$$[A] = [\alpha_1, \alpha_2, \ldots, \alpha_{Nos}]; \quad \alpha_i \in S; \quad i = 1,\ldots,Nos \tag{4}$$

In Eq. (1) to (4), ρ_i is the materials density of the *i*th member, l_i is the length of the *i*th member, a_i is cross section for the *i*th member and Ne is number of structural members. *S* is the list of available profiles found for the numbers of *Ns* from which the optimum designs are chosen. *Nos* is the number of sections for each design which is determined according to structure members grouping. σ_j shows stress value of *j*th member and σ_{all} is the value of allowable stress. Δ_k indicates displacement of *k*th degree of freedom and Δ^{all}_k is maximum displacement of *k*th degree of freedom. *NDOF* is the number of active degrees of freedom for active joints of the structure.

Constraint C1: In an optimum structure, stress raised from load combinations in all members must be in the allowable range which is determined based on code being used. Accordingly, stress value of each member of the structure in optimization process is controlled. Violation of stress constraint is determined by Eq. (5). In *nlc* number of load combinations status, values of constraint violation of all members are added together.

$$C1 = \begin{cases} C_1^i = 0 \ if \left|\dfrac{\sigma_i}{\sigma_{all}}\right| - 1 \le 0 \ ; \ i = 1,\ldots,Ne \\ C_1^i = \left|\dfrac{\sigma_i}{\sigma_{all}}\right| - 1 \ if \left|\dfrac{\sigma_i}{\sigma_{all}}\right| - 1 > 0 \ ; \ i = 1,\ldots,Ne \end{cases} \tag{5}$$

Constraint C2: After structural analysis and calculating the stresses, the displacement of active nodes in each design is calculated. If the *i*th degree of freedom displacement is in the range, no penalty will be considered; otherwise, the design will be penalized proportional to the violation. The violation of the displacement constraint is determined by Eq. (6). In the load combinations status, the violations of the nodal displacement constraints are also added together for *nlc* cases.

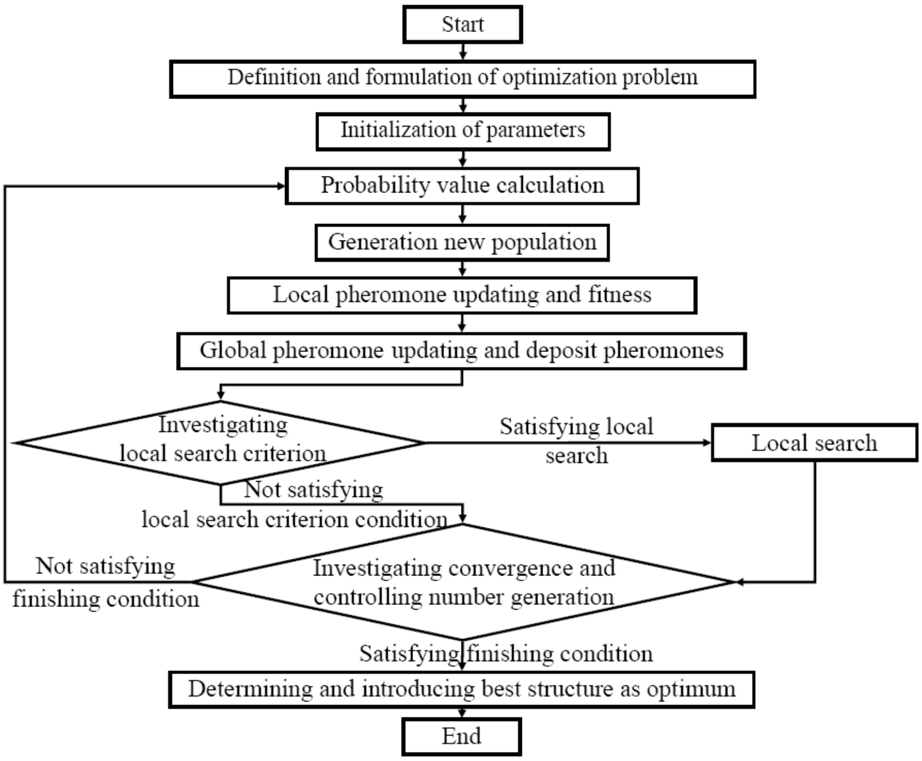

Fig. 1 Structural optimization algorithm by ACO

$$C2=\begin{cases} C_2^i=0 \ \ if \left|\frac{\Delta_i}{\Delta_i^{all}}\right|-1\le 0 \ ; \ i=1,\ldots,Ndof \\ C_2^i=\left|\frac{\Delta_i}{\Delta_i^{all}}\right|-1 \ \ if \left|\frac{\Delta_i}{\Delta_i^{all}}\right|-1>0 \ ; \ i=1,\ldots,Ndof \end{cases} \quad (6)$$

Given that we have all the design information for the problem, the optimization process can be run using any meta-heuristic method. Therefore, the procedure for optimization of structures using the ACO algorithm is conducted as Fig. 1.

2.2 Initialization of Parameters

Similar to other meta-heuristic algorithms, the ACO algorithm also calls for assignment of values to the respective parameters at the beginning. To this end, first, values of the primary parameters such as the number of population members, *α*, *β*, evaporation rate, etc. are set, and then the amount of primary pheromone for all possible status will be initialized. Since there is a choice for the number of sections listed for each member of structures, a matrix called *T* with dimensions proportional to the number of sections from the available list (*NS*) and the number of design variables (number of structural member grouping) will be developed as Eq. (7) to determine the pheromone value.

$$T=\begin{bmatrix} T_{11} & T_{12} & \cdots & T_{1Nos} \\ T_{21} & T_{22} & \cdots & T_{2Nos} \\ \vdots & \vdots & & \\ T_{Ns1} & T_{Ns2} & \cdots & T_{NsNos} \end{bmatrix}_{Ns\times Nos} \quad (7)$$

In this matrix, each element indicates the amount of pheromone rate of the *i*th state from the list of sections for the *j*th design variable. As seen, with increases the number of sections, the design space expands and dimensions of the pheromone matrix grow. These results in a reduction in the convergence speed and increases the probability of getting trapped in local optimum based on ACO. The amount of the primary pheromone in the aforementioned matrix [*T*] is initialized according to Eq. (8).

$$T_{ij}^0=\frac{1}{W_{\min}} \quad (8)$$

Where $W_{\min}$ is the value of the objective function accounted for the first state of the list of sections to all the design variables [17].

2.3 Probability Value Calculation

Following the initialization of the parameters of the combined algorithm, selection probability of each current mode (proportional to sections list) for each design variable is calculated as Eq. (9) [17]:

$$p_{ij}=\frac{\left[T_{ij}\right]^{\alpha}\left[\upsilon_i\right]^{\beta}}{\sum_{k=1}^{Ns}\left[T_{kj}\right]^{\alpha}\left[\upsilon_k\right]^{\beta}} \quad i=1,\ldots,Ns \quad ; \quad j=1,\ldots,Nos \quad (9)$$

Where p_{ij} is the selection probability of the *i*th mode (path) for the *j*th design variable. v_i is the stability coefficient for the *i*th mode from the list of sections which is defined as Eq. (10).

$$\upsilon_i=\frac{1}{a_i} \quad ; \quad a_i\in S \quad ; \quad i=1,\ldots,Ns \quad (10)$$

As can be seen from Eq. (10) the lower the a_i value, the more v_i is and correspondingly p_{ij} increase with the increase of vi according to Eq. (9).

In Eq. (9), α, β are two parameters that weigh the relative importance of the pheromone trail and the heuristic information, respectively. If $\alpha = 0$, then p_{ij} will be proportional to v_i value and correspondingly proportional to the selected cross section value (a_i). Therefore, the optimization process becomes randomized. One the other hand, if $\beta = 0$, then only the pheromone impact will be effective in the choice probability function which can result in a rapid and early convergence and as a consequence, increase the probability of obtaining a local optimum [17].

2.4 Generating New Population

In the ACO algorithm, after calculating the values of the selection probability, new population should be determined based on the p_{ij} value. Since the sum of p_{ij} value for the *j*th design variable is equal to 1, the probability obtained for the *j*th design variable could be illustrated as the circle shown in Fig. 2. The p_{ij} values will form its sectors.

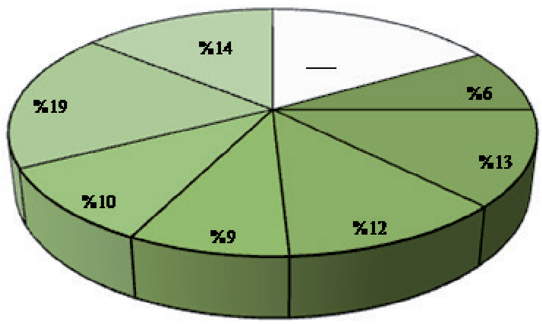

Fig. 2 Probabilities of selection for each design variable

Through generating an additional number between 0 and 1, a cross section from the sections list with larger sectors may have a better chance to be selected. In this method, the cumulative probability of $\overline{P}_i$ for the *j*th design variable is determined as Eq. (11).

$$\overline{P}_i^{\,j} = \sum_{k=1}^{i} P_{kj} \quad ; \quad i = 1, \ldots Ns \tag{11}$$

Then, a random number is produced between 0 and 1. The selected cross section is identified from the list of sections by comparing the random number to $\overline{P}_i^{\,j}$ value. This procedure is performed for all the design variables to from the new design. This process is repeated for all the population to from the new population based on the p_{ij} value according to T_{ij} [1-2].

A close look at the cross section selection scheme for each design variable reveals that with increases the number section, the convergence speed in ACO declines and the chances of being trapped in local optimum has increased. In other words, as seen in Fig. 2, with an increase in the number sections, the number of circle sectors grows. Consequently, the best mode for the *j*th design variable will be slightly different than other possible modes. Hence, too much iteration are required to increase the probability of selection of the best mode proportional to the amount of pheromone and to make a distinction between this mode and other possible modes for the *j*th design variable. Therefore, in ACO increases the number sections plays a significant role in convergence speed and precision of the optimal solution.

2.5 Local Updating and Fitness Calculation

As illustrated in Eq. (12), following new population formation, pheromone rate corresponding to total selected cross section (passed routes) for each design variable is decreased with a constant coefficient which prevents pheromone accumulation on each path and unfavourable and failed decisions are also ignored [17].

$$T_{ij}^{new} = \rho_0 T_{ij}^{old} \tag{12}$$

Where T_{ij}^{new} and T_{ij}^{old} are the *new* and *old* pheromone rates for passed routes, respectively. ρ_0 is the local update coefficient which has a value ranging from 0 to 1.

The value of the objective function, constraint optimization problem is converted to an unconstraint optimization problem which is described by the following equation.

$$\varphi(A) = W(A)\left[1 + K\left(\sum^{nlc}\sum_{q=1}^{Q}\max\left[0, Gq\right]\right)\right] \tag{13}$$

Where $W(A)$ is the objective function, G_q is the structural violation rate related to each constraint, Q is the total constraints governing the problem and K is the penalty function. As can be deduced from Eq. (13), for every design that violates the problem constraints more, the corresponding ϕ value will be more as well and will have lower fitness [18]. As a result, following the estimation of ϕ values corresponding to each design, the present population will be ranked merit-based.

2.6 Global updating and depositing pheromones

After ordering the present population based on fitness, the pheromone rate of all modes in the list of sections for all the design variables at global upgrading stage are decreased with coefficient called evaporation rate. In the other words, all the pheromone matrix entries are reduced based on the following equation [17].

$$[T]^{new} = (1 - e_r)[T]^{old} \tag{14}$$

Where e_r indicates the pheromone global evaporation rate. *old* and *new* transcribers indicate old and new pheromone matrixes, respectively.

After performing the global pheromone evaporation process, pheromone should be placed on the passed routes. In the present work, a small population, λ_r, of the best present population (μ) is primarily formed. λ_r value is initialized at the first stage. Afterwards, pheromone rate of the list of sections modes for design variables which are selected in the selection stage (passed routes) is increased as Eq. (15) [17].

$$T_{ij} = T_{ij} + e_r \cdot \left[\lambda_r \cdot \left(\Delta T_{ij} \right)_{best} + \sum_{k=1}^{\lambda_r} \left(\lambda_r - r_k \right) \cdot \left(\Delta T_{ij} \right)_k \right] \tag{15}$$

Where ij indicates the passed routes and r_k shows each design number in μ population so that r_k is always in the range of 1 to λ_r. $(\Delta T_{ij})_k$ represents the amount of pheromone needed to be placed in the ij route which depends on resulted response quality raised from kth design and (ΔT_{ij}) best corresponds to the best design. (ΔT_{ij}) for kth design is calculated as Eq. (16).

$$\left(\Delta T_{ij} \right)_k = \frac{1}{\varphi(A)^k} \tag{16}$$

Where $\phi(A)$ for the kth design based on Eq. (13) is among the best. Considering Eq. (15), more pheromone is placed on the passed routes from μ population which results in an increase of the convergence rate in the present algorithm [17].

2.7 Search in the neighborhood of best design

In this paper, if no change is observed in successive generation of the optimization process in fitness value of the best population design, this process is performed. Each element of any pheromone matrix column indicates a cross-section of the list of sections. The list has been sorted from the smallest to the biggest cross-section. On the other hand, each element of any pheromone matrix row indicates a design variable. Therefore, it is possible to specify the pheromone matrix element related to the best design. In this step, the elements of the best design and two/three upper and lower elements of the optimum design are considered equal to the initial pheromone rate. The remaining elements of pheromone matrix are considered equal to zero. In other words, corresponding to some members of list of sections in the upper and lower of the variable of optimum design in pheromone matrix, pheromone is considered equal to the primary pheromone value. Investigations indicated that this process has a considerable effect on improving the performance of ACO [7, 11].

2.8 Termination criterion

Several methods are available for termination condition in meta-heuristic algorithm [19]. In this paper, termination condition is satisfied with controlling the number of iterations. After termination of the algorithm, the best design obtained as the optimum design, and the convergence curve is drawn.

3 Proposal Idea

As mentioned in the previous section, in the ant colony algorithm, with the growth of the number of sections, the probability of reaching a local optimum increases while the convergence speed declines. In this paper, inspired by the meshing process in the finite element method for the analysis of different structures, it was tried to discrete the design space such that each design variable situate in appropriate range of the design space being searched. To this end, first the list of sections forming the problem design space should be divided into a number of subsets. The number of subsets and members of each subset are determined by user's choice in proportion to the sections listed as well as the problem and structure conditions. In the next step, one member of the subset is selected as the representative. To this end, three possible cases were assumed in this paper. In the first, second and third cases, the largest cross sectional, the medium cross sectional, and the smallest cross sectional in each subset were selected as the representatives of each section, respectively. In any event, after determining the representatives of each subset, the list of new sections for all design variables is created. This list includes the representatives of each subset. Therefore, each design variable uses the new list of sections for selecting a cross sectional. That is to say, the list of sections for the optimization problem is turned into a new list with fewer members than the initial list through the portioning process. The reduction in the number of section increases the convergence speed.

After determining the list of sections, the optimization process starts based on ACO as described in Section 2. In this phase, since the list of sections only contains the representatives of each subset, the optimization procedure is carried out based on a global search. That is to say, in this phase, the optimal design range for each design variable is identified through a global search based on a new list of sections. The optimization process in this phase continues for a predetermined number of iterations. In this paper, the criterion was considered equal to half the total number of assumed generation procedures. As a result, the algorithm has enough time to run the global search process. It is worth mentioning that this criterion may vary depending on the problem and structure conditions.

At the end of the generation procedure related to global search, the local search process is run based on ACO. For this purpose, the list of sections for each design variable changes in proportion to the optimal design resulted from the global search process. In other words, the optimal design values resulted from the global search represent a selected subset of the list of sections. Hence, each design variable only uses the new list of sections around the result of the global search process. Evidently, the list of sections for each design variable is different and has fewer members than initial list of problem. In any event, after determining the new list of sections for each design variable, the optimization process continues based on the procedure used

Table 1 Dividing members of the list of sections into 8 subsets for examples 1, 2 and 3

	Subset (1) - S1			Subset (2) - S2			Subset (3) - S3			Subset (4) - S4	
No.	in²	mm²	No.	in²	mm²	No.	in²	mm²	No.	in²	mm²
1	0.111	71.613	1	0.602	388.386	1	1.457	939.998	1	2.630	1696.771
2	0.141	90.968	2	0.766	494.193	2	1.563	1008.385	2	2.880	1858.061
3	0.196	126.451	3	0.785	506.451	3	1.620	1045.159	3	2.930	1890.319
4	0.250	161.290	4	0.994	641.289	4	1.800	1161.288	4	3.090	1993.544
5	0.307	198.064	5	1.000	645.160	5	1.990	1283.868	5	3.380	2180.641
6	0.391	252.258	6	1.130	729.031	6	2.130	1374.191	6	3.470	2238.705
7	0.442	285.161	7	1.228	792.256	7	2.380	1535.481	7	3.550	2290.318
8	0.563	363.225	8	1.266	816.773	8	2.620	1690.319	8	3.630	2341.931
	Subset (5) - S5			Subset (6) - S6			Subset (7) - S7			Subset (8) - S8	
No.	in²	mm²	No.	in²	mm²	No.	in²	mm²	No.	in²	mm²
1	3.840	2477.414	1	4.970	3206.445	1	11.500	7419.430	1	19.900	12838.684
2	3.870	2496.769	2	5.120	3303.219	2	13.500	8709.660	2	22.000	14193.520
3	3.880	2503.221	3	5.740	3703.218	3	13.900	8967.724	3	22.900	14774.164
4	4.180	2696.769	4	7.220	4658.055	4	14.200	9161.272	4	24.500	15806.420
5	4.220	2722.575	5	7.970	5141.925	5	15.500	9999.980	5	26.500	17096.740
6	4.490	2896.768	6	8.530	5503.215	6	16.000	10322.560	6	28.000	18064.480
7	4.590	2961.284	7	9.300	5999.988	7	16.900	10903.204	7	30.000	19354.800
8	4.800	3096.768	8	10.850	6999.986	8	18.800	12129.008	8	33.500	21612.860

in Section 2. In this phase, searching continues around the optimal design resulted from the previous search phase. That is to say, the design space is explored based on ACO in two phases by establishing a logical balance between the global and local search processes.

4 Numerical Examples

In order to evaluate the performance of the proposed idea in different cases, examples of the optimization of skeletal structures are considered. On the other hand, the following steps were taken to demonstrate the method of application of the proposed idea. First, the list of sections for examples 1, 2 and 3 was assumed based on [18, 20] (Table 1 without divisions and with 64 members). Afterwards, based on the proposed idea, the list of sections was divided into eight subset with 8-member as shown in Table 1.

It is worth mentioning that this classification is changeable by problem conditions, and the list of section is changeable by user's choice, but in this paper the same classification was assumed for examples 1, 2 and 3. Another important point regarding this process is that sorting of the list of sections was carried out from the lowest section to the highest section. That is to say, before dividing the list of section, it is necessary to perform an ascending sort on the members of the primary set. In the following, according to the proposed cases, the initial list of sections for all of the design variables is formed in each case based on the representatives of each subset. To this end, in *Case* 1, the largest member of the set is selected as the representative. In *Case* 2, the middle member of the set is selected as the representative, and in *Case* 3 the smallest member is selected as the representative. Therefore, the list of sections at the beginning of optimization process for each of the proposed cases is as follows:

S - *Case* 1 = {366.225, 816.773, ..., 12129.008, 21612.86}

S - *Case* 2 = {198.064, 645.16, ..., 9999.980, 17096.74}

S - *Case* 3 = {71.613, 388.386, ..., 7419.430, 12838.684}

By changing the list of sections in each case, the number of sections declines drastically, and this decrease has a considerable effect on the optimization process. In the following, as described in Section 3, at the end of the global search, the list of sections for each design variable changes in proportion to the results and in accordance with Table 1. Consequently, the local search process starts. Since in the local search phase the number of sections for each design variable is eight, the number of sections in this phase is far lower than that of the initial list. In this section, several examples are optimized for evaluating the efficiency of the proposed idea in the assumed cases. It shall be mentioned that to avoid the effect of random parameters on the optimization process, the convergence diagrams for each case in each example are drawn using an average of 40 different runs. For this purpose, in each example, based on an ant colony algorithm named S-ACO, first the optimization process was carried out in accordance with section 2. Then, the examples were optimized based on proposed idea and the optimization process was carried out in the proposed cases (*Case* 1, *Case* 2 and *Case* 3). Finally, the convergence path to attain an optimum point is used as a criterion for comparison of the above mentioned cases and S-ACO.

Table 2 Loading conditions for the 47-bar steel tower

P kips (kN)	Condition 1		Condition 2		Condition 3	
	17	22	17	22	17	22
X	6 (26.689)	6 (26.689)	6 (26.689)	--	--	6 (26.689)
Y	-14 (-62.275)	-14 (-62.275)	-14 (-62.275)	--	--	-14 (-62.275)

4.1 A 47-bar steel tower

A 47-bar tower, shown in Fig. 3, has been evaluated as the first example. Here, E and ρ are assumed to be as 30000 *ksi* (206842.8 *MPa*) and 0.3 lb/in^3 (8303.97 kg/m^3), respectively. According to the symmetry of structure, the structural members are categorized into 27 groups and the allowable compressive and tensile stresses for all members are considered as 15 *ksi* (103.4214 *MPa*) and 20 *ksi* (137.895 *MPa*), respectively.

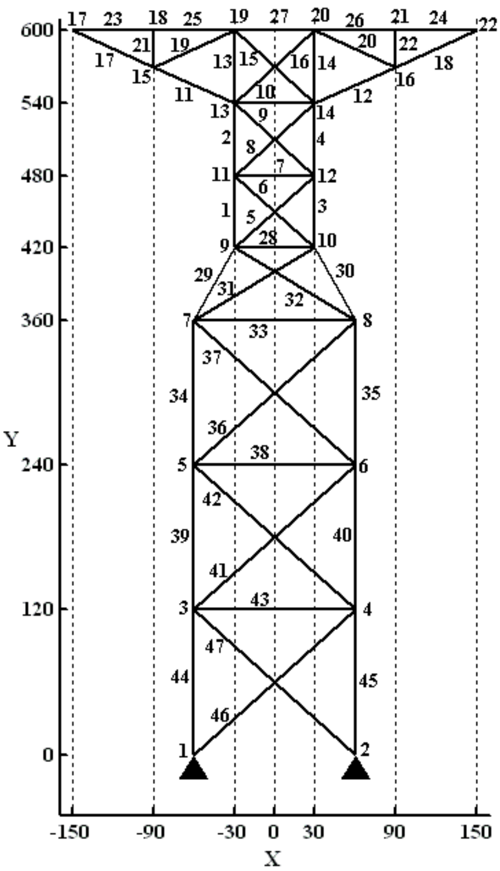

Fig. 3 A 47-bar steel tower

On the other hand, allowable buckling stress for each member was controlled according to reference [20] as shown in Eq. (17).

$$\sigma_i^{cr} = -\frac{kEA_i}{L_i^2} \quad i = 1, ..., 47 \tag{17}$$

Where k buckling constant is intended 3.96. It is worth noting that the structure is subjected to three loading conditions as shown in Table 2.

This example was examined using different proposed cases as well as the S-ACO method. Fig. 4 shows the convergence trend graph for this example in *Cases* 1, 2 and 3 as well as the S-ACO. Each curve is obtained using the average of 40 different runs. Therefore, to obtain the curves in Fig. 4, a total of 160 independent runs were created. As seen, the second proposed case (*Case* 2) has better convergence than the other cases in obtaining the optimum design. Moreover, this case lead to lighter weight than the other existing cases. Table 3 includes the results of the optimum design for *Case* 2 as compared to other references.

Table 3 Optimal design comparison for the 47-bar steel tower - (mm^2)

No.	[20] HS	This Study Case 2	No.	[20] HS	This Study Case 2
1	2477.414	2477.414	15	939.998	939.998
2	2180.641	2180.641	16	285.161	363.225
3	494.193	641.289	17	2341.931	2341.931
4	90.968	71.613	18	939.998	939.998
5	506.451	506.451	19	252.258	161.290
6	1283.868	1283.868	20	1993.544	1993.544
7	1374.191	1374.191	21	939.998	792.256
8	792.256	792.256	22	126.451	198.064
9	1008.385	1008.385	23	2477.414	2477.414
10	1374.191	1374.191	24	1008.385	1008.385
11	71.613	71.613	25	126.451	90.968
12	71.613	90.968	26	2961.284	2961.284
13	1161.288	1161.288	27	939.998	939.998
14	1161.288	1161.288	***W* - *kg***	**1087.17**	**1081.499**

4.2 A 52-bar truss

In this example, the optimal design of a 52-bar truss, shown in Fig. 5, is performed. Here, E and ρ are considered as 2.07×10^5 *MPa* and 7860 kg/m^3, respectively.

In Fig. 5, the loads P_x , P_Y are 100 *kN* and 200 *kN*, respectively. Here, the truss members are categorized into 12 groups and the allowable stress constraints are considered in range of ±180 *MPa*.

Different proposed cases and S-ACO were applied to the optimal design of this truss. Fig. 6 shows the convergence curves obtained by S-ACO and different proposed cases. From this figure it can be deduced that *Case* 2 is more successful and also possesses a higher chance of obtaining lighter designs than the other proposed cases and references. Table 4 includes the results of the optimum design of other references compared to those of the second proposed case (*Case* 2).

Table 4 Optimal design comparison for the 52-bar truss structure - (mm^2)

Gr.	Mem.	[21] GA	[20] HS	[22] HPSO	[23] DHPSACO	[7] RBASLU,2	[24] CSS	This Study Case 2
1	A_1-A_4	4658.055	4658.055	4658.055	4658.055	4658.055	4658.055	4658.055
2	A_5-A_{10}	1161.288	1161.288	1161.288	1161.288	1161.288	1161.288	1161.288
3	A_{11}-A_{13}	645.160	494.193	363.225	494.193	506.451	388.386	494.193
4	A_{14}-A_{17}	3303.219	3303.219	3303.219	3303.219	3303.219	3303.219	3303.219
5	A_{18}-A_{23}	1045.159	939.998	940.000	1008.385	940.000	940.000	939.998
6	A_{24}-A_{26}	494.193	641.289	494.193	285.161	506.451	494.193	494.193
7	A_{27}-A_{30}	2477.414	2238.705	2238.705	2290.318	2238.705	2238.705	2238.705
8	A_{31}-A_{36}	1045.159	1008.385	1008.385	1008.385	1008.385	1008.385	1008.385
9	A_{37}-A_{39}	285.161	363.225	388.386	388.386	388.386	494.193	506.451
10	A_{40}-A_{43}	1696.771	1283.868	1283.868	1283.868	1283.868	1283.868	1283.868
11	A_{44}-A_{49}	1045.159	1161.288	1161.288	1161.288	1161.288	1161.288	1161.288
12	A_{50}-A_{52}	641.289	494.193	792.256	506.451	506.451	494.193	494.193
	C_i	--	--	--	0.002725	0.000116	0.001143	--
	Weight-*kg*	1970.142	1903.36	1905.495	1904.83	1899.35	1897.62	1903.183

Table 5 Loading conditions for the 72-bar truss structure

Node	Condition 1			Condition 2		
	P_x kips (kN)	P_y kips (kN)	P_z kips (kN)	P_x kips (kN)	P_y kips (kN)	P_z kips (kN)
17	5.0 (22.241)	5.0 (22.241)	-5.0 (-22.241)	0	0	-5.0 (-22.241)
18	0	0	0	0	0	-5.0 (-22.241)
19	0	0	0	0	0	-5.0 (-22.241)
20	0	0	0	0	0	-5.0 (-22.241)

Table 6 Optimal design comparison for the 72-bar truss structure - (mm^2)

Element Group	[21] GA	[23] DHPSACO	[24] CSS	[18] MSM	[11] HACOHS-T	[25] CS	This Study Case 2
A_1-A4	126.451	1161.288	1283.868	1283.868	1008.385	1161.288	1374.191
A5-A12	388.386	285.161	285.161	388.386	363.225	363.225	363.225
A13-A16	198.064	90.968	71.613	71.613	71.613	71.613	71.613
A17-A18	494.193	71.613	71.613	71.613	71.613	71.613	71.613
A19-A22	252.258	792.256	641.289	816.773	816.773	816.773	792.256
A23-A30	252.258	363.225	363.225	285.161	363.225	363.225	285.161
A31-A34	90.968	71.613	71.613	71.613	71.613	71.613	71.613
A35-A36	71.613	71.613	71.613	71.613	71.613	71.613	71.613
A37-A40	1161.288	363.225	363.225	285.161	252.258	363.225	285.161
A41-A48	388.386	363.225	363.225	388.386	363.225	285.161	363.225
A49-A52	90.968	71.613	71.613	71.613	71.613	71.613	71.613
A53-A54	198.064	161.290	71.613	71.613	71.613	71.613	71.613
A55-A58	1008.385	126.451	126.451	126.451	126.451	126.451	126.451
A59-A66	494.193	363.225	363.225	363.225	363.225	388.386	363.225
A67-A70	90.968	285.161	285.161	252.258	252.258	252.258	252.258
A71-A72	71.613	363.225	494.193	285.161	388.386	0363.225	363.225
Weight- kg	193.776	178.434	178.284	177.63	176.983	176.842	176.806

4.3 A 72-bar truss

This example deals with optimization of a 72-bar truss, as illustrated in Fig. 7. Here E and ρ are assumed to be 10000 *Ksi* (68947.6 *MPa*) and 0.1 lb/in^3 (2767.99 kg/cm^3), respectively.

Stress range for the truss members and the maximum nodal displacement are limited to ±25 *ksi* (±172.369 *MPa*) and ±0.25 *in* (0.635 *Cm*), respectively. Present truss members are categorized into 16 groups. Table 5 shows the applied loads the structures in two different conditions.

Fig. 8 shows the convergence curves of the present truss as an average of 40 different runs based on proposed cases and S-ACO.

As it is shown in this figure, the second proposed case (*Case* 2) has a better average performance and lead to lighter weight than the other existing cases. Table 6 includes the results of the optimum design for the *Case* 2 and some other existing approaches.

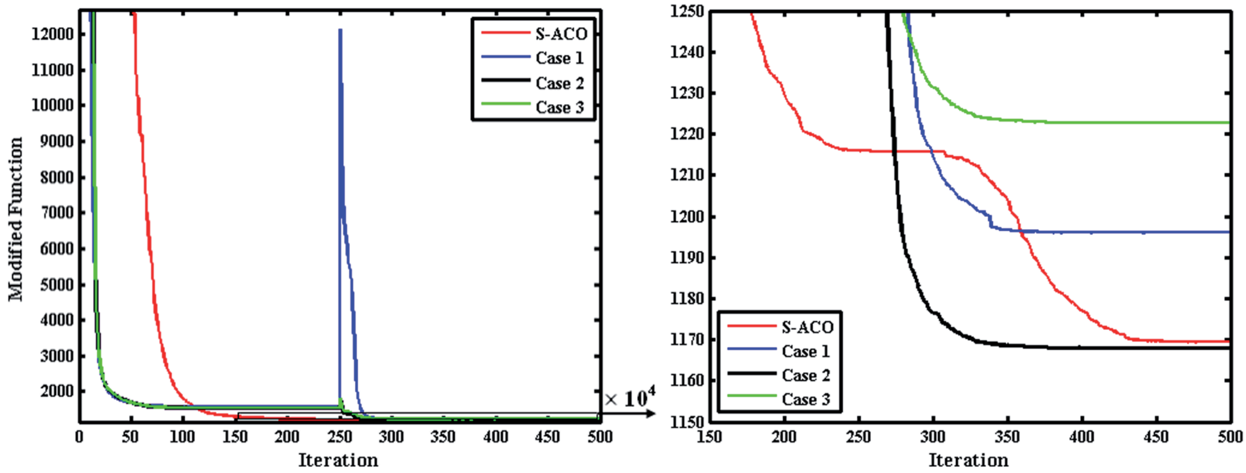

Fig. 4 The convergence history of the proposed cases and S-ACO for the 47-bar steel tower

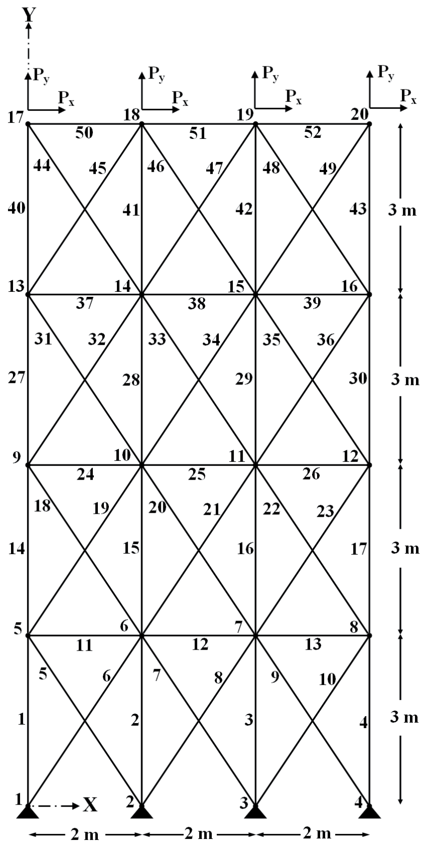

Fig. 5 A 52-bar planar truss structure

4.4 An eight-story, one-bay frame

As the last example, the optimization of an eight-story frame with one bay, as illustrated in Fig. 9, is considered.

For all the frame members, E and ρ are assumed as 200 *GPa* and 76.8 kN/m^3, respectively, and the lateral drift at the top of the structure is the only performance constraint (limited to 5.08 *cm*). Effective loads are considered for one condition as shown in Fig. 9. Members of the mentioned frame are categorized into 8 groups selected from a list of 268-sections (Table 7) [26].

In this example, to apply the proposed idea, members of the list of section are divided into 33 subset with eight members and one 4-member subset after sorting the list of section, (Table 8).

As a result, in the global search phase for the proposed idea, the list of sections consists of a total of 34 members. Each subset is defined in proportion to each case as following, and the resulting list contains fewer sections than the initial list.

S - *Case* 1 = {W6 × 12, W12 × 16, …, W36 × 848}

S - *Case* 1 = {W10 × 12, W6 × 15, …, W14 × 730}

S - *Case* 1 = {W6 × 9, W4 × 13, …, W40 × 593}

This example was also examined for different proposed cases as well as S-ACO method. In Fig. 10, the convergence curves for this example are illustrated for present cases. This confirms that the convergence rate of the second proposed case (*Case* 2) is higher. The best design for the present frame is also obtained by *Case* 2.

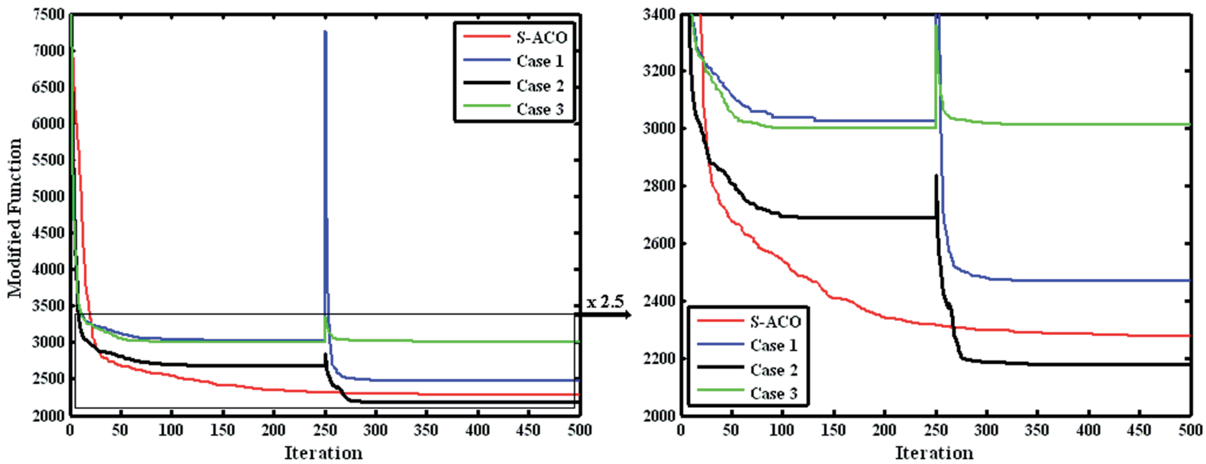

Fig. 6 The convergence history of the proposed cases and S-ACO for the 52-bar truss structure

Table 7 The available cross-section areas of the AISC W-Section

No.	Section	A - cm²	Ix - cm⁴	Sx - cm³	Iy - cm⁴	S_y - cm³
1	W44 × 335	634.1923	1294479.734	23105.76	49947.771	2458.059
2	W44 × 290	553.5473	1127987.163	20319.959	43704.299	2179.479
267	W5 × 16	30.1934	886.573	139.454	312.589	20.811
268	W4 × 13	24.7096	470.341	89.473	160.665	16.387

Table 8 Dividing members of the list of sections into 34 subset

Subset (1) - S1	Subset (2) - S2	Subset (3) - S3	⋯	Subset (32) - S32	Subset (33) - S33	Subset (34) - S34
W6 × 9	W4 × 13	W6 × 16		W14 × 370	W40 × 466	W40 × 593
W8 × 10	W8 × 13	W10 × 17		W40 × 372	W30 × 477	W14 × 605
⋮	⋮	⋮		⋮	⋮	⋮
W10 × 12	W5 × 16	W6 × 20		W27 × 448	W27 × 539	W14 × 808
W6 × 12	W12 × 16	W8 × 21		W14 × 455	W14 × 550	W36 × 848

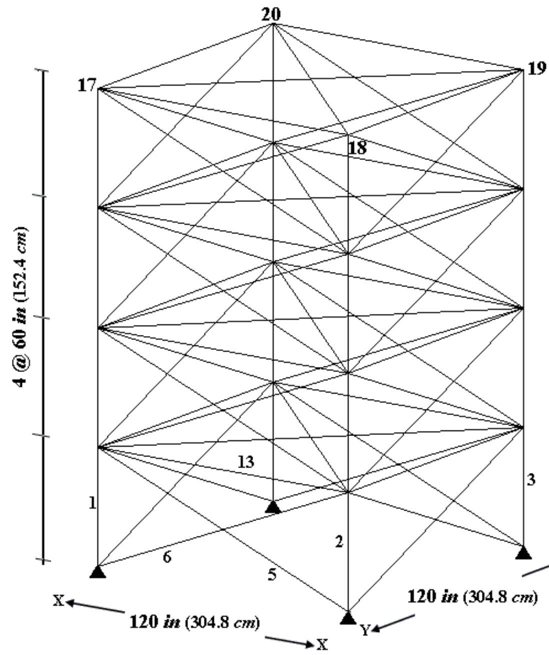

Fig. 7 A 72-bar truss structure

Optimal design resulting from the *Case* 2 and also the results from other references are presented in Table 9. The resulting convergence trend graph and optimal design indicate acceptable suitable performance of the *Case* 2.

5 Conclusions

In the present study, inspiring meshing process in finite element method, design space of the optimization problem is divided into different parts. Hence, value of each design variable is explored in an appropriate range. To this purpose, optimization process is started based on the new list of sections by interpretation of global search. Then, following determining appropriate range of design variable, local search process is performed and resulting values of optimal design are determined. Consequently, optimization problem will be assessed based on the proposed idea through establishing a logical balance between global search process and local search process like other state of the art ACO methods.

To implement this idea, first the list of available sections was divided into several subsets and the representative of each subset was defined as the new list of sections for the global search process. To achieve this goal, the new list of sections was formed using the representatives of each subset in three cases. In *Case* 1, *Case* 2, and *Case* 3, the largest, median, and smallest

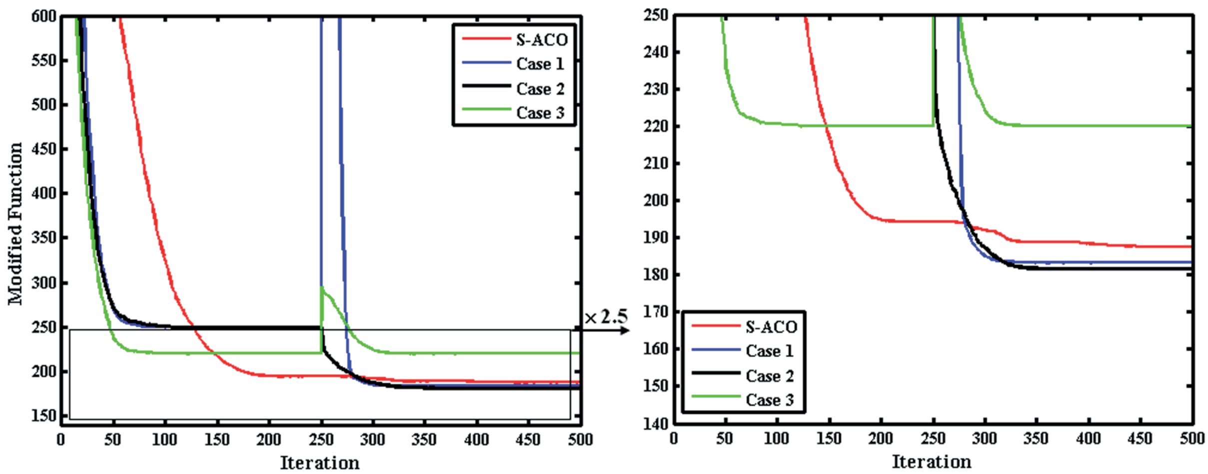

Fig. 8 The convergence history of the proposed cases and S-ACO for the 72-bar truss structure

Table 9 Optimal design comparison for the one-bay, eight story frame

Gr.	[27] GA	[28] FEAPGEN	[6] ACO	[29] HGAPSO	[9] ACO	[30] DPSACO	This Study Case 2
1	W14 × 34	W18 × 46	W21 × 50	W18 × 35	W18 × 40	W18 × 35	W 21 × 44
2	W10 × 39	W16 × 31	W16 × 26	W18 × 35	W16 × 26	W16 × 31	W 16 × 26
3	W10 × 33	W16 × 26	W16 × 26	W14 × 22	W16 × 26	W16 × 26	W 14 × 22
4	W8 × 18	W12 × 16	W12 × 14	W12 × 16	W12 × 14	W14 × 22	W 12 × 16
5	W21 × 68	W18 × 35	W16 × 26	W16 × 31	W21 × 44	W16 × 31	W 18 × 35
6	W24 × 55	W18 × 35	W18 × 40	W21 × 44	W18 × 35	W18 × 40	W 18 × 35
7	W21 × 50	W18 × 35	W18 × 35	W18 × 35	W18 × 35	W16 × 26	W 18 × 35
8	W12 × 40	W16 × 26	W14 × 22	W16 × 26	W12 × 22	W14 × 22	W 16 × 26
w-*kN*	41.02	32.83	31.68	31.243	31.05	30.91	30.83

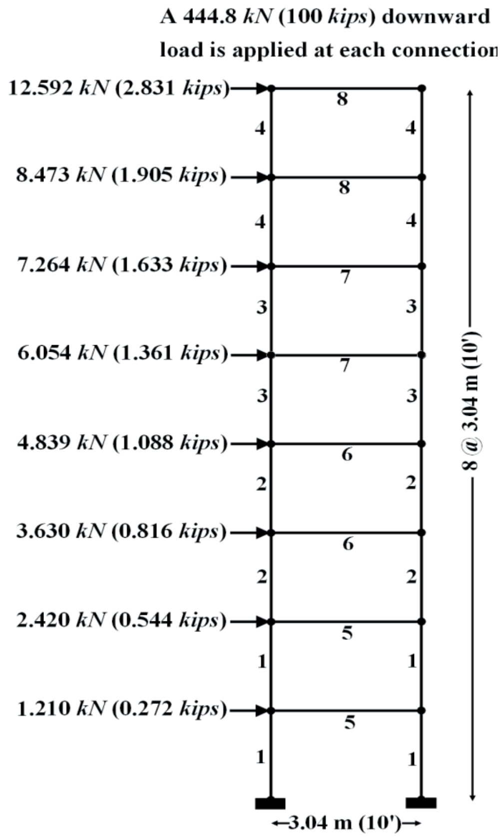

Fig. 9 A one-bay eight-story frame structure

cross-sectional areas of each subset were selected as the representatives, respectively. Following the formation of the new list of sections, the optimization process continued until the last global search condition was satisfied. The list of sections for each design variable was then identified in accordance with the results of the global search phase, and the optimization process based on ACO continued around the result. Consequently, the second phase reflected the local search process around the suitable design resulted from the previous phase.

This proposed idea in ACO increases the convergence speed and improves the results. This is shown in convergence curves of Fig. 4, Fig. 6, Fig. 8 and Fig. 10, each of which shows the results of 160 independent runs of the optimization process. As seen in these figures, after the algorithm enters the local search phase in the proposed cases, the convergence trend graph shows a drastic decline, which reflects the rapid advancement of the algorithm toward the optimal design. Particularly, *Case* 2 of the proposed idea demonstrates a suitable trend in moving toward the optimum design in all of the examples.

Applicability of this proposed for other meta-heuristic algorithms are underlined as its obvious characteristic. On the other words, improving the performance of other meta-heuristic algorithms such as ACO, PSO, CSS, etc. is an effectual feature of this proposed.

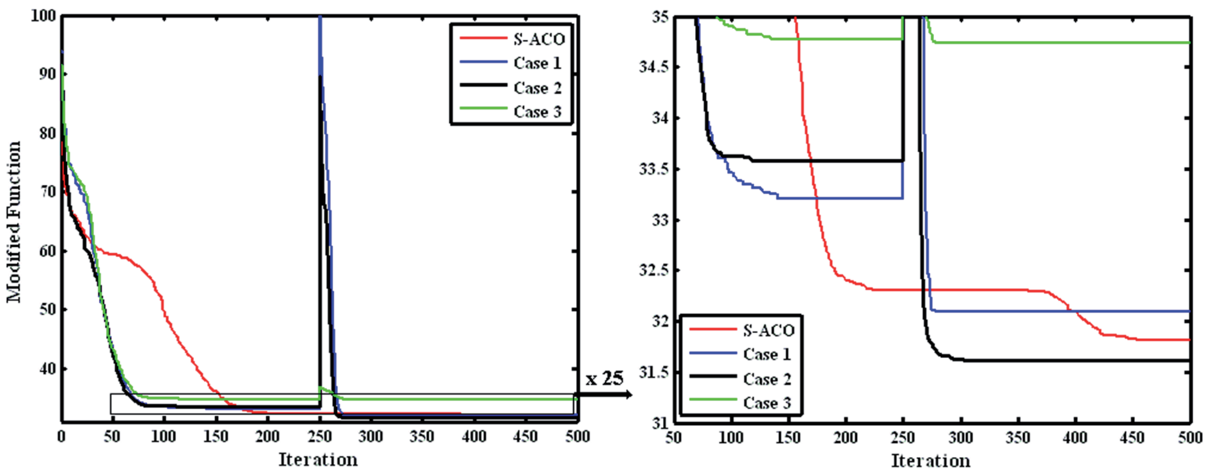

Fig. 10 The convergence history of the proposed cases & S-ACO for the one-bay, 8 story frame

References

[1] Camp, C. V., Bichon, B. J. "Design of space trusses using ant colony optimization." *Journal of Structural Engineering*. 130(5), pp. 741-751. 2004. DOI: 10.1061/(ASCE)0733-9445(2004)130:5(741)

[2] Camp, C. V., Bichon, B. J., Stovall, S. P. "Design of steel frames using ant colony optimization." *Journal of Structural Engineering.* 131(3), pp. 369-379. 2005. DOI: 10.1061/(ASCE)0733-9445(2005)131:3(369)

[3] Colorni A, Dorigo M, Maniezzo V. "Distributed optimization by ant colonies." In: Proceedings of the First European Conference on Artificial Life, Paris, France, Dec. 11-13. 1991. pp. 134-142. URL: http://s3.amazonaws.com/academia.edu.documents/4418203/ic.06-ecal92.pdf?AWSAccessKeyId=AKIAJ56TQJRTWSMTNPEA&Expires=14773-92338&Signature=nHIfFQgfyoevmK6%2Fh6%2BklChQCqU%3D&response-content-disposition=inline%3B%20filename%3DDistributed_optimization_by_ant_

[4] Dorigo M. Optimization Learning and natural algorithm. PhD. thesis, Dipartimento di Elettronica, Politecnico di Milano, 1992. (in Italian).

[5] Csébfalvi, A. Angel method for discrete optimization problems. *Periodica Polytechnica Civil Engineering*. 51(2), pp. 37-46. 2007. DOI: 10.3311/pp.ci.2007-2.06

[6] Kaveh, A., Shojaee, S. "Optimal design of skeletal structures using ant colony optimization." *International Journal for Numerical Methods in Engineering*. 70(5), pp. 563-581. 2007. DOI: 10.1002/nme.1898

[7] Capriles, P. V. S. Z., Fonseca, L. G., Barbosa, H. J. C., Lemonge, A. C. C. "Rank-based ant colony algorithms for truss weight minimization with discrete variables." *Communications in Numerical Methods in Engineering.* 23(6), pp. 553-575. 2007. DOI: 10.1002/cnm.912

[8] Csébfalvi, A., "A hybrid meta-heuristic method for continuos engineering optimization." *Periodica Polytechnica Civil Engineering*. 53(2), pp. 93-100. 2009. DOI: 10.3311/pp.ci.2009-2.05

[9] Kaveh, A., Talatahri, S. "An improved ant colony optimization for the design of planar steel design frames." *Engineering Structures*. 32(3), pp. 864-873. 2010. DOI: 10.1016/j.engstruct.2009.12.012

[10] Csébfalvi, A. "Multiple constrained sizing-shaping truss-optimization using ANGEL method." *Periodica Polytechnica Civil Engineering*. 55(2), pp. 81-86. 2011. DOI: 10.3311/pp.ci.2011-1.10

[11] Talebpour, M. H., Kaveh, A., Kalatjari, V. R. "Optimization of skeletal structures using a hybridized ant colony-harmony search-genetic algorithm." *Iranian Journal of Science and Technology, Transaction of civil engineering.* 38(C1), pp. 1-20. 2014. URL: http://ijstc.shirazu.ac.ir/article_1840_ad8eb554563ff7b30715cd9d974537ec.pdf

[12] Kaveh, A., Kalatjari, V. R., Talebpour, M. H. "Optimal design of steel towers using a multi-metheuristic based search method." *Periodica Polytechnica Civil Engineering.* 60(2), pp. 151-178. 2016. DOI: 10.3311/PPci.8222

[13] Stützle, T., Hoos, H. "Improvement on the Ant-System: Introducing MAX-MIN ant system." In: *Artificial Neural Nets and Genetic Algorithms.* Proceedings of the International Conference in Norwich, U.K., 1997. (Ed. Smith, G. D., Steele, R. F.) pp. 245-249. 1997. DOI: 10.1007/978-3-7091-6492-1_54

[14] Bullnheimer B, Hartl RF, Strauss C. A new rank-based version of the ant system: a computational study, Technical Report POM-03/97, Institute of Management Science, University of Vienna, 1997.

[15] Cordón, O., Herrera, F., Stützle, T. "A review on ant colony optimization metaheuristic: basic, models and new trends." *Mathware & Soft Computing*. 9(2-3), pp. 1-35. 2002. URL: http://natcomp.liacs.nl/SWI/papers/ant.colony.optimization/A.Review.on.the.Ant.Colony.Optimization.Metaheuristic-Basis.Models.and.New.Trends.pdf

[16] Barbosa, H. J. C. (ed.) "*Ant Colony Optimization - Techniques and Applications"* InTech, 2013. DOI: 10.5772/3423

[17] Hasançebi, O., Çarbaş, S., Doğan, E., Erdal, F., Saka, M. P. "Performance evaluation of meta-heuristic search techniques in the optimum design of real size pin jointed structures." *Computers & Structures*, 87(5-6), pp. 284-302. 2009. DOI: 10.1016/j.compstruc.2009.01.002

[18] Kalatjari, V. R., Talebpour, M. H. "Sizing and topology optimization of truss structures by modified multi-search method." Journal of Civil and Surveying Engineering, 45(3), pp. 351-363, 2011.

[19] Dreo, J., Petrowski, A., Siarry, P., Taillard, E. "*Metaheuristic for hard optimization.*" Springer-verlag, Berlin, Heidelberg, 2006.

[20] Lee, K. S., Geem, Z.W., Lee, S-H., Bae, K. W. "The harmony search heuristic algorithm for discrete structural optimization." *Engineering Optimization*. 37(7), pp. 663-684. 2005. DOI: 10.1080/03052150500211895

[21] Wu, S-J., Chow, P-T. "Steady-state genetic algorithm for discrete optimization of trusses." *Computers and Structures.* 56(6), pp. 979-991. 1995. DOI: 10.1016/0045-7949(94)00551-D

[22] Li, L.J., Huang, Z. B., Liu, F. "A heuristic particle swarm optimization method for truss structures with discrete variables." *Computers & Structures*. 87(7-8), pp. 435-443. 2009. DOI: 10.1016/j.compstruc.2009.01.004

[23] Kaveh, A., Talatahari, S. "A particle swarm ant colony optimization for truss structures with discrete variables." *Journal of constructional steel research*. 65(8-9), pp. 1558-1568. 2009. DOI: 10.1016/j.jcsr.2009.04.021

[24] Kaveh. A., Talatahri, S. "A charged system search with a fly to boundary method for discrete optimum design of truss structures." *Asian Journal of Civil Engineering (Building and Housing)*. 11(3), pp. 277-293. 2010. URL: http://www.sid.ir/en/VEWSSID/J_pdf/103820100301.pdf

[25] Kaveh, A., Bakhshpoori, T. "Optimum design of space trusses using cuckoo search algorithm with Levy flights." *Iranian Journal of Science and Technology, Transaction of Civil Engineering.* 37(C1), pp. 1-15. 2013.

[26] American Institute of Steel Construction (AISC), Manual of steel construction-allowable stress design, 9th ed, American Institute steel construction, Chicago, 1998.

[27] Khot, N S., Venkayya, V. B., Berke, L. "Optimum structural design with stability constraints." *International Journal for Numerical Methods in Engineering*. 10(5), pp. 1097-1114. 1976. DOI: 10.1002/nme.1620100510

[28] Camp, C.V., Pezeshk, S., Cao, G. "Optimized design of two dimensional structures using a genetic algorithm." *Journal of Structural Engineering*. 124(5), pp. 551-559. 1998. DOI: 10.1061/(ASCE)0733-9445(1998)124:5(551)

[29] Kaveh, A., Malakoutirad, S. "Hybrid genetic algorithm and particle swarm optimization for the force method-based simultaneous analysis and design." *Iranian Journal of Science and Technology, Transaction B: Engineering*. 34(B1), pp. 15-34. 2010.

[30] Kaveh, A., Talatahari, S. "A discrete particle swarm ant colony optimization for design of steel frames." Asian journal of Civil Engineering (Building and Housing). 9(6), pp. 563-575. 2007.